JOURNAL OF AIRCRAFT
Vol. 40, No. 3, May–June 2003

Design of a Martian Autonomous Rotary-Wing Vehicle

Anubhav Datta,* Beatrice Roget,* Daniel Griffiths,* Gregory Pugliese,*
Jayanarayanan Sitaraman,* Jinsong Bao,* Lin Liu,* and Olivier Gamard*
University of Maryland, College Park, Maryland 20742

The design of a Martian autonomous rotary wing vehicle (MARV) is described. MARV is a 50-kg gross takeoff mass, coaxial helicopter designed for Mars exploration. Powered by a fuel cell system, it carries a payload of 10.8 kg over a range of 25 km with an endurance of 39 min including hover capability for 1 min. MARV is designed in response to the Request For Proposal from NASA/Sikorsky for the Year 2000 American Helicopter Society student design competition. The design covers aerodynamic and structural design of rotor blades, vehicle power plant, fuselage and landing gear, control system, transmission, and vehicle lander communications. A detailed mechanism for autonomous deployment of the vehicle from the lander is also described. This preliminary design study indicates that controlled vertical flight on Mars is feasible with existing technology.

Introduction

A ROTORCRAFT can be a perfect platform for Mars exploration. It can take off and land from unprepared sites avoiding launch and recovery challenges of fixed-wing explorers. It has greater speed, range, and field of view than a surface rover. It can hover and fly at low speeds and survey hostile terrains more closely than an orbiter. Its ability to return to a precise landing spot opens opportunity for recharging and flying multiple missions. It can return samples from remote sites to the lander platform. Thus, it combines the benefits of a surface rover and an air vehicle.

The potential benefits of using a vertical lift platform for planetary exploration are identified by Young et al.[1] and Young.[2] They discuss the technical aspects of vertical lift planetary aerial vehicles in general and examine notional vehicles for Mars, Titan, and Venus exploration. An early work on the feasibility of a rotary-wing configuration for Mars is reported by Savu et al.[3] The solar cell performance assumed in this paper, which focused on the powerplant, requires realistic reassessment after the Pathfinder mission. The present Martian autonomous rotary wing vehicle (MARV) design has been described in detail in Ref. 4.

Critical Design Issues

The Martian atmosphere generates unique design problems. Table 1 shows a comparison of the key planetary properties of Earth and Mars. A 20% reduced value of density is considered to make the design robust to unforeseen changes in atmospheric conditions. Gravity is 3 times lower on Mars but atmospheric density is 100 times lower. Therefore, the rotor blades operate at very high blade loading. Combination of Martian density and viscosity generates Reynolds numbers 0.019 times that on Earth. The speed of sound is 0.7 times that on Earth. Thus, a very low Reynolds number flow is encountered with a severely restricted Mach number ceiling. Lack of oxygen and low atmospheric pressure requires an unconventional power plant. Additional challenges are posed by the requirement of transporting the vehicle to Mars. Transportation ease calls for a simple design, easy to fold and easy to deploy. Lack of satellites in orbit, repeater stations on ground, and any significant ionosphere to bounce off signals require a suitable vehicle lander communications system.

Received 10 April 2002; revision received 21 November 2002; accepted for publication 18 December 2002.

*Graduate Research Assistant, Alfred Gessow Rotorcraft Center, Department of Aerospace Engineering.

MARV Configuration

The Request For Proposal specifies a maximum takeoff mass of 50 kg. It specifies the following as required mission elements. 1) autonomous deployment, 2) 30 min of controlled flight, 3) 25-km range (preferable), 4) 1-min hover, and 5) optional restart capability. Within the constraints posed by the critical design issues, a preliminary estimate of payload using the Boeing–Vertol formula (see Ref. 5) shows (Fig. 1) that a vehicle with 50-kg takeoff mass maximizes both payload and payload fraction for such a mission. Moreover, the fundamental low Reynolds number problem argues for as large a vehicle as possible. Therefore, the vehicle takeoff mass is fixed as 50 kgs. A comparative study of 15 different helicopter configurations reveals that a conventional single rotor-tail rotor, a coaxial configuration, and a quadrotor are the most controllable configurations on Mars (Fig. 2).

The coaxial configuration is selected for the following reasons. Because of a large rotor radius and a long tail rotor arm, the folding and deployment of a single rotor configuration is very complex. A coaxial configuration, with two rotors, generates the required thrust with a smaller disk area and needs no antitorque device. A quadrotor, a configuration with four rotors each with its own revolutions per minute control, produces blade chord Reynolds numbers of 2×10^4. It is found that, below Reynolds numbers of 5×10^4, turbulent separation can keep an airfoil permanently stalled on Mars. For the same overall size, a coaxial rotor can be designed to maintain chord Reynolds numbers over 5×10^4. Moreover, the lower profile drag of coaxial rotor blades operating at higher Reynolds numbers increases lift-to-drag ratios and offers higher payload capability. Finally, compared to a quadrotor, coaxial technology is more mature. Hence, a coaxial configuration is selected. A two-bladed coaxial configuration is preferred over a three-bladed one because higher chord Reynolds numbers generate lower profile drag.

Four views of the final MARV configuration are shown in Fig. 3.

Detailed Mission Segments

Once the vehicle takeoff mass and configuration are selected, detailed mission calculations can be performed. The basic mission profile is shown in Fig. 4 and described in Table 2.

An initial deployment procedure frees the helicopter from the lander and performs preflight system checks. Following go-ahead from mission control on Earth, the rotor blades are spun to full revolutions per minute using power from the lander. Once the rotors are spun up, the helicopter's internal power source takes over. An initial vertical liftoff of 5 m is performed to clear the lander antenna. This is followed by acceleration to the maximum forward speed of 11.5 m/s (22 kn). Climb to an altitude of 100 m in 37 s follows. The climb rate is limited to one-third of the maximum value to ensure that the airfoils do not stall. Cruise is performed at 100-m altitude followed by descent, which proceeds to a height of 10 m above

the ground. The descent rate is the same as climb rate. Following a full deceleration, the MARV hovers for 60 s at a height of 10 m (out of ground effect). It then executes a soft landing in 10 s. The basic mission lasts for 39 min, covers a range of 25 km, and consumes 3025 W·h (1 W·h = 3.6 kJ) of energy. An extended mission of 3-min duration covers a distance of 197 m and requires 242 W·h of energy. It begins with a restart of the rotor, followed by a short vertical takeoff, acceleration and climb, cruise, deceleration and descent, and landing phase. The total energy required to perform both missions is 3267 W·h. An alternate sample-return mission can be one in which MARV flies out a distance, collects a soil sample, and returns to the lander. With the same amount of energy, the range for a sample-return mission is 13.34 km with no hover segment. A long-range reconnaissance mission can be performed with the available scientific payload replaced by more energy capacity to fly to a distance of 120 km one way.

Rotor Aerodynamic Design

Compared to conventional missions on Earth, aerodynamic design is more critical to the success of a Martian mission. Energy considerations on Mars demand a large rotor diameter with minimum hover power. Packaging and weight considerations dictate that rotor diameter be as small as possible. Producing the required lift with a minimum rotor disk area generates a very high tip Mach number in the Martian atmosphere. High drag at low Reynolds number ($<5 \times 10^5$) dictates a low solidity for low profile power. Thus, the already high blade loading due to low atmospheric density becomes even more severe. To support a high blade loading, Reynolds number must be maximized, which means higher tip speeds or higher solidity. These are unconventional and conflicting requirements.

Table 1 Comparison of atmospheric properties

Properties	Earth	Mars	Design value
Gravity (g), m/s^2	9.81	(0.373 g) 3.66	3.66
Pressure (p), Pa	1.0135*e*5	(0.0078 p) 790.53	632.42
Temperature, K	288.16	210.56	210.56
Density (ρ), kg/m^3	1.225	(0.0136 ρ) 0.0167	0.0133
Viscosity (μ), kg/ms	1.789*e*−05	(0.721 μ) 1.289*e*−05	1.289*e*−05
Molecular gas constant (R), J/kg·K	287	(0.67 R) 192	192
Adiabatic coefficient (γ)	1.4	(0.92 γ) 1.29	1.29
Speed of sound (a), m/s	320	(0.72 *a*) 230	230

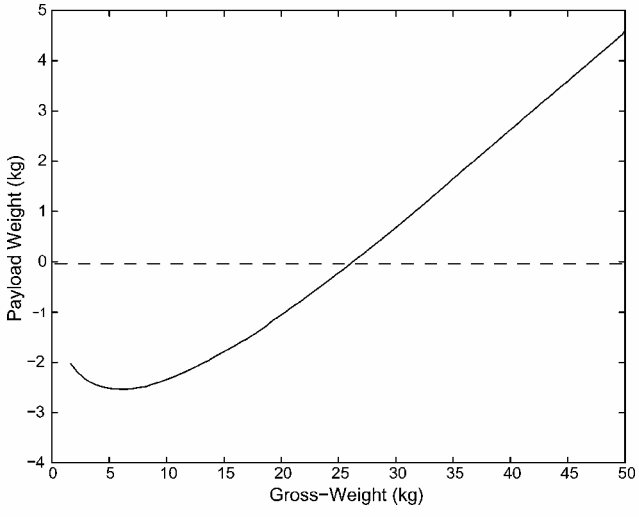

Fig. 1 Preliminary payload estimation using Boeing-Vertol formulae.

Rotor Planform Design

The planform is designed to produce a favorable Reynolds number distribution over the entire flight envelope while avoiding adverse compressibility effects. The Reynolds number and Mach number distributions over the span of the MARV blade are shown in Fig. 5. Reynolds numbers of at least 5×10^4 are maintained over 60% of the span. Maximum Reynolds number of 8×10^4 occurs at 80% span. In the present study, it was noted that below a Reynolds number of 5×10^4 it is very difficult to keep the turbulent boundary layer attached to the airfoil. High Mach number and high lift conditions lead to sonic flow or strong pressure gradients that separate the weak boundary layer quickly and stall the airfoil.

The rotor planform is shown in Fig. 6. A parabolic tip sweep in the outer 20% of the blade allows the inboard sections to operate at higher Reynolds number while keeping the incident Mach number below 0.5. The sweep at the extreme tip reaches 37 deg. The rotor radius is 7 ft. This is the smallest radius at which the required blade loading can be achieved with the desired Reynolds number and Mach number distributions. Also it keeps the aspect ratio slightly greater than 4. Below 4, adverse three-dimensional flow effects can lead to performance degradation. From a root cutout of 10 to the 40% radial station, the blade is split into three inverse taper sections. The inverse tapers benefit blade folding and also help to keep the required lift coefficients below the stall limit. Between the 40 and 80% radius, the blade tapers with a ratio of 1.2. Taper increases effective aspect ratio and decreases profile power. Lift drops off near the tip so that the chord Reynolds number can be lowered at the tip by decreasing the chord and to save structural weight. The blade planform resembles propeller blades as shown in Fig. 6. The Pathfinder blade, which operates at low Reynolds numbers (one order higher than MARV), has a similar planform distribution. All three propeller blades shown in Fig. 6 have low aspect ratios and operate at high thrust, similarly to the blades used on MARV.

Table 2 Details of basic mission segments

Description	Duration	μ	Distance	Average power, kW	Energy required, W·h
Rotor spinup	——	0	0	——	0
Takeoff to 5 m	30 s	0	0	5.369	47.73
Acceleration	60 s	0–0.08	345 m	4.74	79
Climb to 100 m	38 s	0.08	437 m	4.6	53.41
Cruise	2040 s	0.08	23459 m	4.6	2607
Descent to 10 m	36 s	0.08	414 m	4.6	41.4
Deceleration	60 s	0.08–0	345 m	4.74	79
Hover	60 s	0	0	4.88	81.33
Landing	30 s	0	0	4.392	36.6
Total	39.23 min	——	25 km	——	3025.47

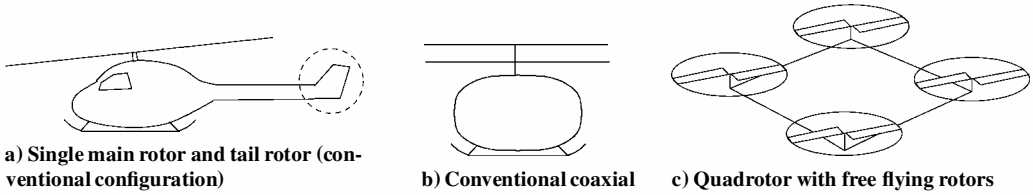

a) Single main rotor and tail rotor (conventional configuration) **b) Conventional coaxial** **c) Quadrotor with free flying rotors**

Fig. 2 Conventional main rotor-tail rotor, coaxial configuration, and quadrotor configuration.

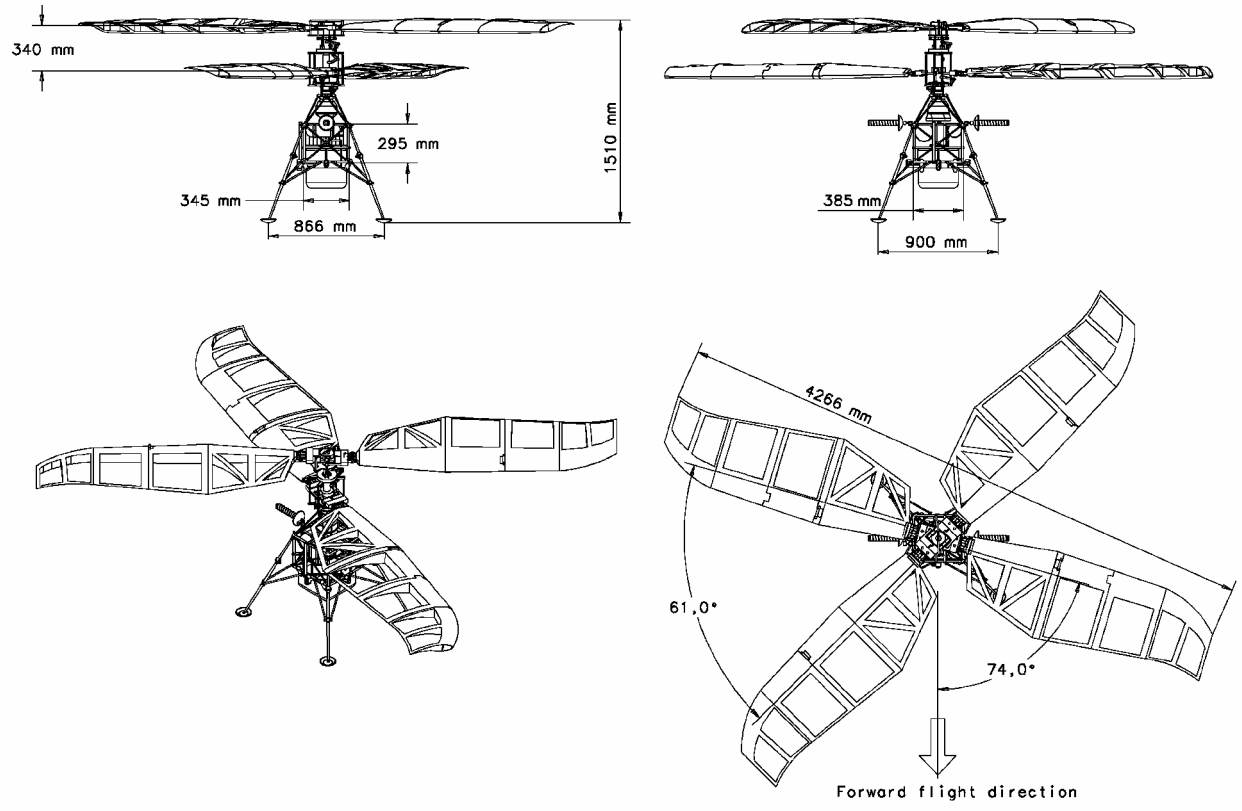

Fig. 3 Four views of MARV.

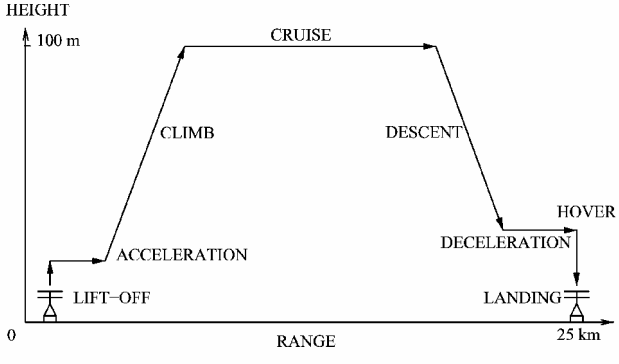

Fig. 4 Basic mission profile.

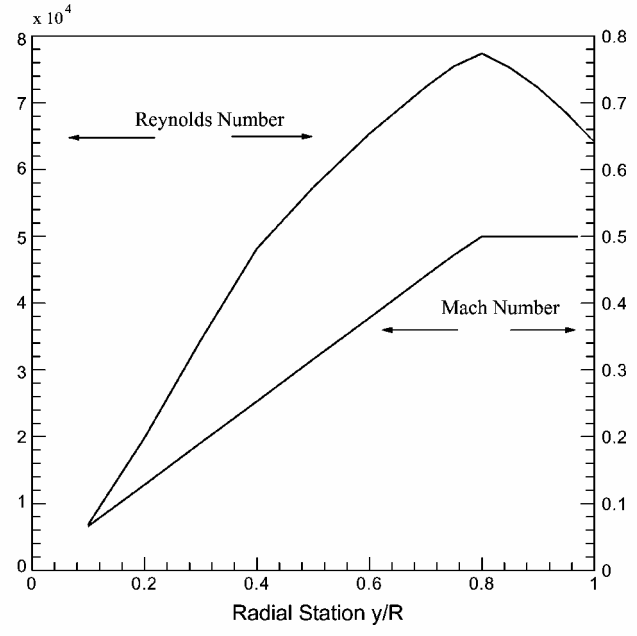

Fig. 5 Reynolds number and Mach number distribution on MARV blades in hover.

Airfoil Design

The extensive University of Illinois at Urbana–Champaign (UIUC) low-speed airfoil test data show that airfoils can be designed to operate at high lift and low Reynolds number (6×10^4–1×10^5) (Ref. 6). However all of these tests were performed at low subsonic speeds. Using airfoil coordinates and lift data from the UIUC database, an inviscid, incompressible panel method is used to estimate pressure distributions around the airfoils at high Mach numbers. All airfoils show very low critical Mach numbers. Critical Mach numbers first appear at the retreating blade because of high lift and not on advancing blade because of high speed. The flow on the retreating blade accelerates to sonic conditions due to the steep pressure drop near the leading edge. Appearance of a shock completely separates the flow and very little useful lift is generated.

When sonic flow is prevented, a high adverse pressure gradient separates the boundary layer. Between Reynolds numbers of 6×10^4 and 1×10^5, wind-tunnel tests[6] show that the laminar boundary layer separates before transition to turbulence. Turbulent reattachment downstream creates a laminar separation bubble. A laminar separation bubble can increase drag by 200%. In the present study, it is observed that at high Mach numbers (0.4–0.5) turbulent reattachment does not occur and the flow remains fully separated. Below 6×10^4, even a fully turbulent flow separates against pressure gradients at high lift conditions at the given Mach number regime. Other existing low Reynolds number airfoils such as the Apex 16 used in the NASA high-altitude flight experiments[7] operate at Reynolds numbers 2–10 times higher than MARV. In general, none of the existing low Reynolds number airfoils is directly applicable to MARV.

Airfoil AGRC 1506, shown in Fig. 7, is designed to meet the described challenges. AGRC 1506 has a maximum thickness of 15%

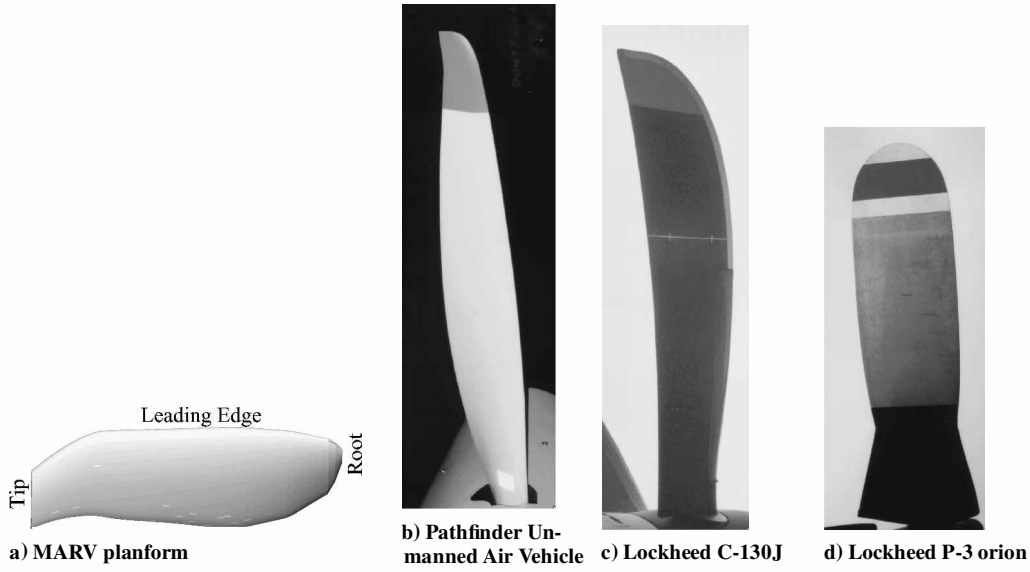

a) MARV planform

b) Pathfinder Unmanned Air Vehicle

c) Lockheed C-130J

d) Lockheed P-3 orion

Fig. 6 Rotor planform.

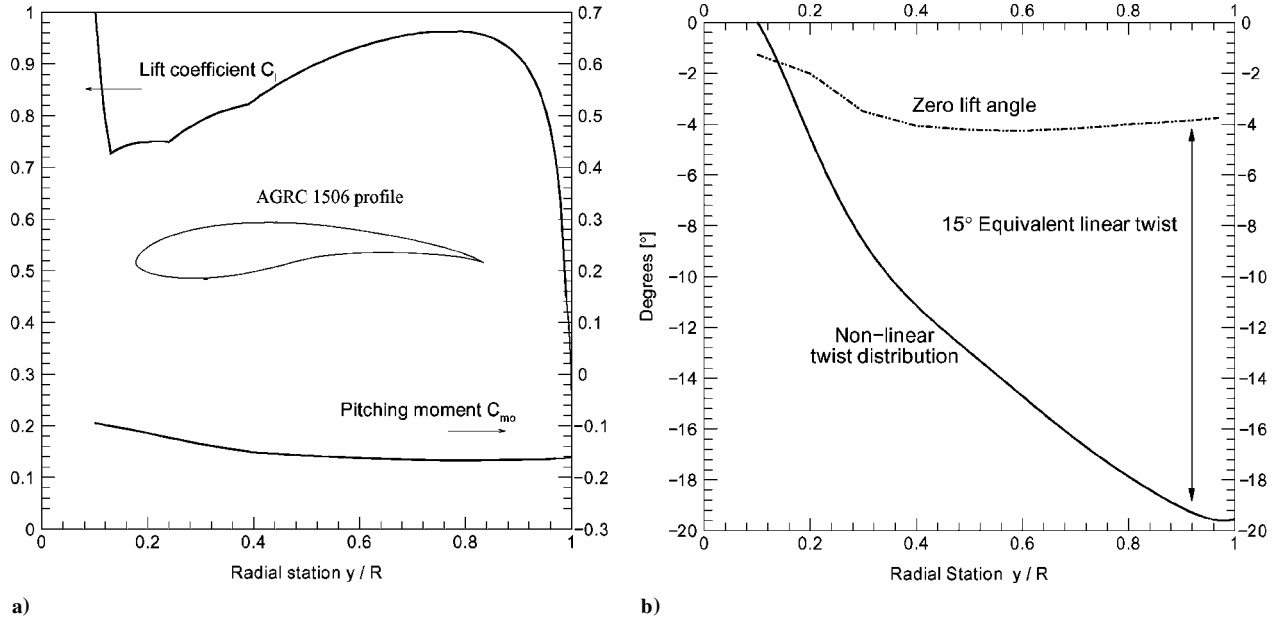

a) b)

Fig. 7 Airfoil AGRC 1506: a) section lift and pitching moment coefficients in hover and b) spanwise twist distribution.

chord and a maximum camber of 6% chord. High camber does not generate high control loads on Mars due to the very low dynamic pressure. Trips are used in AGRC 1506 at 40 and 20% chord on upper and lower surface to trigger turbulent boundary layers and to prevent the formation of a laminar separation bubble. To prevent turbulent separation, camber is distributed to spread the lift over a larger area of the airfoil and, thus, prevent steep pressure gradients at the leading edge. Below a Reynolds number of 5×10^4, it becomes extremely difficult to keep the turbulent layer attached. Hence, chord Reynolds numbers on the MARV blade are kept greater than 5×10^4 for 60% of the span. The design is performed using the Xfoil commercial airfoil design program.[8] The lift and pitching moment coefficient distributions along the blade in hover are shown in Fig. 7. Critical conditions at the retreating blade side still limit the forward flight speed. The power curve in Fig. 8 shows that forward speed is determined by airfoil performance, not power considerations.

The advance ratio set for forward flight is 0.08 (11.5 m/s or 22 kn). This keeps adequate margins for gusts of 5 m/s. Figures 9 and 10 show a comparison of AGRC 1506 performance with the rotor operating envelope in hover and forward flight. Figure 9 shows that the lift coefficients required at sections operating at a given Mach

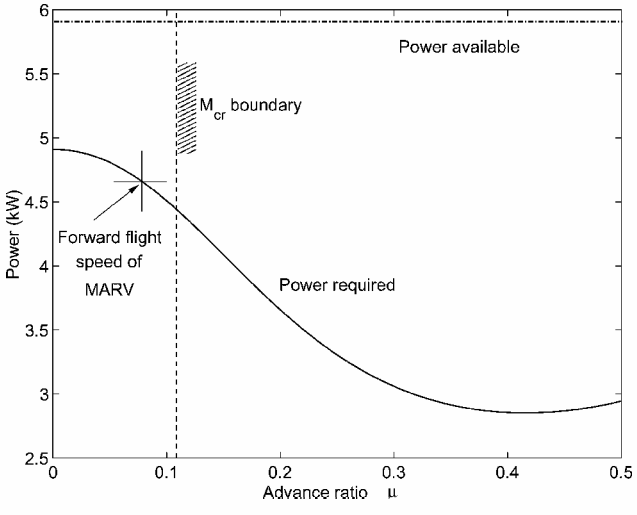

Fig. 8 Power required in forward flight.

Table 3 Characteristics of MARV rotor

Characteristic	Value
Number of blades	2 per rotor
Radius	2.13 m (7 ft)
Maximum chord	0.670 m (2.2 ft)
Tip chord	0.366 m (1.2 ft)
Tip speed	143.75 m/s (471.6 ft/s)
Tip Mach number	0.625 (effectively 0.5)
Thrust-weighted solidity (each rotor)	0.1585
Effective chord	0.530 m (1.74 ft)
Thrust coefficient (each rotor)	0.0232
Disk loading (each rotor)	1.75 kg/m^2 (0.135 lb/ft^2)
Power loading	10.2 kg/kW (6.29 lb/hp)
Blade loading	0.1464
Mean lift coefficient	0.85
Maximum blade Reynolds number	7.8×10^4
Tip Reynolds number	6.48×10^4
Hover power required	4880 W (6.54 hp)
Forward flight power required ($\mu = 0.08$)	4620 W (6.19 hp)

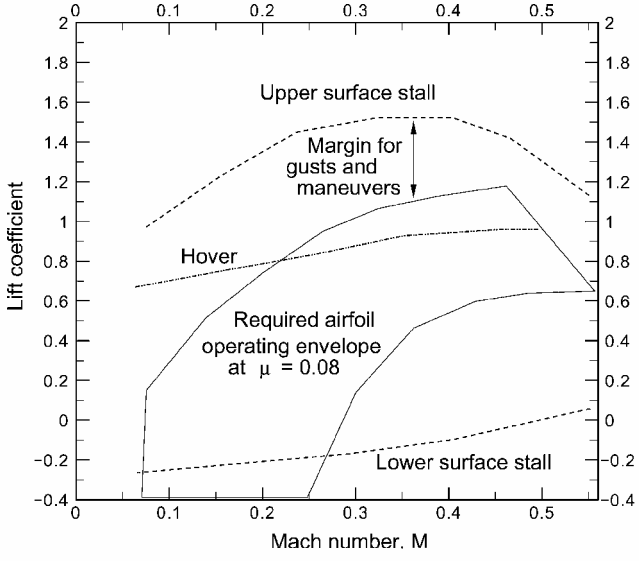

Fig. 9 Lift–Mach number envelope for MARV blades.

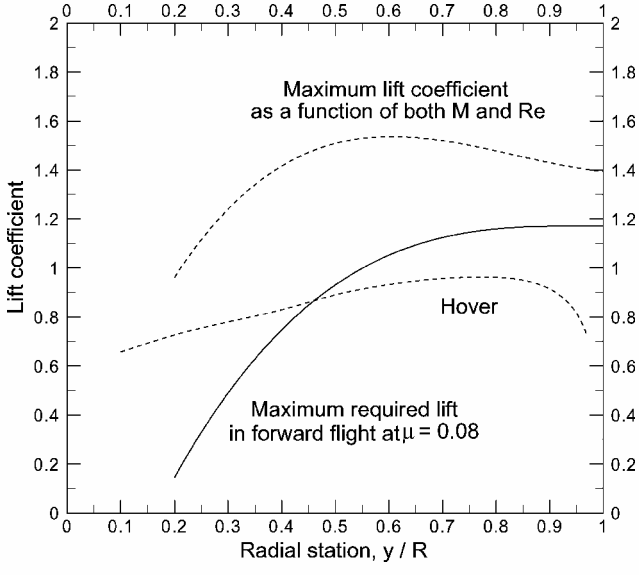

Fig. 10 Maximum lift at each radial station on MARV blade.

number have adequate stall margin for gusts. Figure 10 shows that the maximum lift requirement at any section in hover or forward flight is well within the airfoil limits. Finally, the MARV rotor characteristics are summarized in Table 3. The forward flight power includes rotor power, fuselage drag, and power for onboard systems. The combinations of MARV disk loading and power loading follows established trends, as shown in Fig. 11, where vehicles on Earth have been shifted to Martian conditions. Figure 11 includes the hypothetical NASA planetary aerial vehicle.[1]

Rotor Structural Design

Figure 12 shows a MARV blade. A single box beam spar with transverse rib structures constitutes the frame. Wrapped all around is ultra-thin Mylar® skin.[9] The weight of the rotor blade is used as the objective function to determine the thickness of the spar, I beams, ribs, and the trailing-edge structure. To prevent aeroelastic instabilities, the center of gravity of the rotor blade is constrained to coincide with the quarter-chord location. Section A–A′ (Fig. 12) shows the typical section of a rib. The bending loads from the lifting forces are supported by the I beam, whereas the Nomex honeycomb core and side plates preserve the shape and support torsion. Sections B–B′ and C–C′ show the spar structure. The spar is supported by a leading-edge piece at the front (which brings the c.g. to quarter chord) and by an I beam at the rear.

MARV's coaxial rotors have teetering hubs. A large chord makes MARV rotors stiff. A teetering hub reduces the vertical vibratory loads. The first elastic flap frequency is 1.15 per revolution. In-plane lag frequency is high, 3.6 per revolution. Because the rotor is stiff in-plane, there is no possibility of ground or air resonance. The low forward flight speed along with low aerodynamic loading generates low in-plane vibratory loads. Avionics and imaging instruments are isolated from rotor loads using a vibration absorber described in the gear-box design section.

Power Plant Design

Seven energy options are analyzed and compared for the MARV power plant. For this study, it is assumed that the mission requires 3000 W·h of energy with hover power of 6 kW and rotor torque of 127 N·m.

Hydrazine Fueled Engines

The best value of specific fuel consumption (SFC) that is attained with the current state of implementation is 0.99 kg/MJ. The lowest theoretical value achievable is 0.67 kg/MJ (Ref. 10). When an engine weight of 10 kg is assumed, total power plant weight (engine and fuel) of 20.7 and 17.24 kg are obtained using the preceding SFC.

Hydrazine-Powered Tip Jet Propulsion

When a specific impulse of 300 s (Ref. 10) is assumed, 26.5 kg of fuel is required for a tip jet propulsion scheme. However, the specific impulse assumed is possible only with a very high adiabatic combustion temperature (3410 K) and pressure [1000 psi (6.89 MPa)] (Ref. 11) leading to a very high engine weight.

Concept of CO_2-Breathing Propulsion Engine

Recently, the feasibility of a CO_2-breathing engine using the metal fuels aluminum and magnesium has been assessed in Japan.[12] However, this technology is not yet developed.

Electrical Power from Batteries

The type of batteries that are needed for powering a Martian helicopter fall in the category of vehicle traction batteries, with high-energy density and high-power density. Lithium primary cells are the state of the art among the non-rechargeable batteries. The Pathfinder Rover used lithium thionyl chloride primary cells to handle peak loads and as a power system backup. Lithium thionyl chloride cells can deliver energy densities of 500 W·h/kg by the use of halogen additives.[13] However, power density is extremely limited, which makes them incapable of vehicle traction. The most promising of the batteries for vehicle traction are lithium ion rechargeable cells.

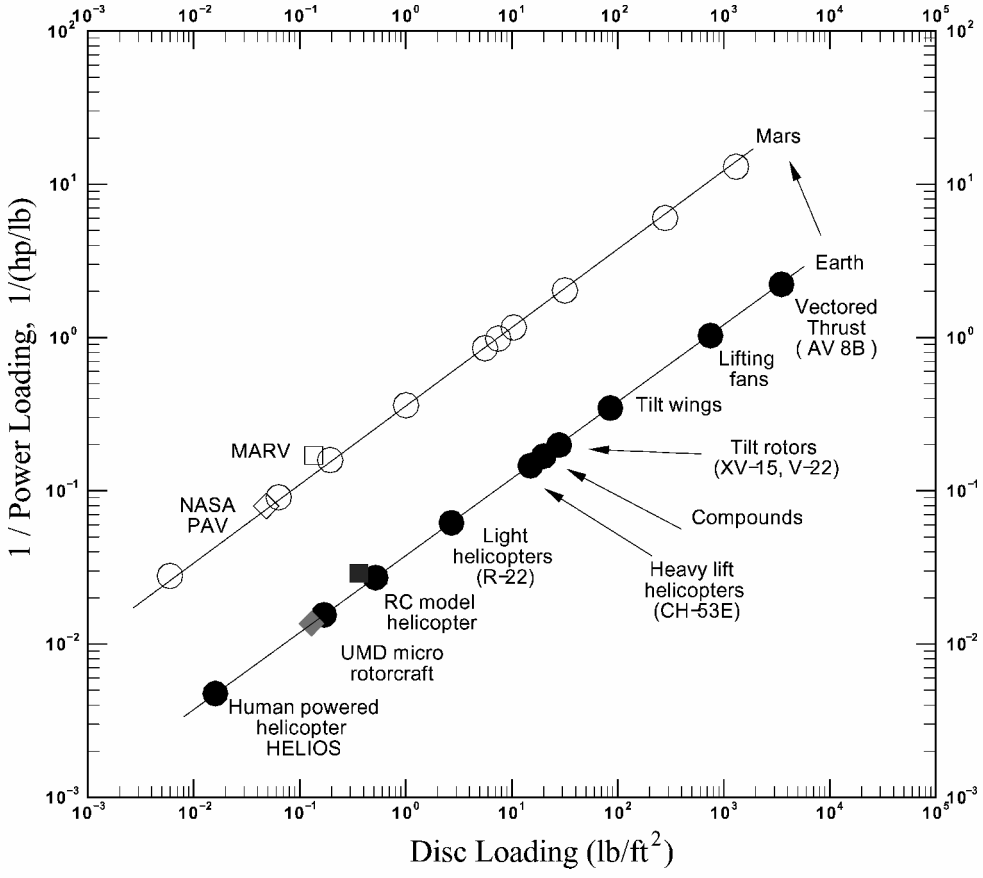

Fig. 11 Disk loading vs inverse of power loading for powered-lift aircraft on Earth and Mars.

A lithium ion battery currently manufactured by SAFT (France) has an energy density of 150 W·h/kg and power density of 300 W/kg. Using these values requires a battery mass of 20 kg. The volumetric power density value is 250 W·h/dm^3. Hence, it takes only 12 dm^3 of space inside MARV. The forecast values for lithium ion vehicle traction batteries for the year 2006 are energy densities near 200–220 W·h/kg and volumetric energy densities of around 400 W·h/dm^3 (Ref. 13). With an energy density value of 220 W·h/kg, the 13.6 kg of battery mass would be sufficient.

Electric Power from Solar Cells

Two figures of merit measure the performance of a solar array power system: power generated per unit mass in watts per kilogram (specific power) and power generated per unit area in watts per square meter (power density). Current state-of-the-art Si cells on rigid panels used in space have recorded values of 30–40 W/kg and 90–110 W/m^2. Advanced flexible lightweight solar arrays can produce 130 W/kg and 90–110 W/m^2 (Ref. 14). When these values are assumed for Mars, 46 kg of solar cells and 55 m^2 of solar cell area is required during flight. Given the rotor disk area is 14.3 m^2, such a scheme is clearly infeasible. Moreover, specific power and density values are much lower on Mars because of much lower solar intensity (590 W/m^2). The Mars Pathfinder rover recorded values of only 5 W/kg and 45 W/m^2 with GaAs/Ge cells. However, the Pathfinder lander cells generated energy at the rate of 3888 kJ/day, which is 1080 W·h/day (Ref. 15). At this rate, the mission energy of 3267 W·h can be collected in a little over three days. This energy can then be used to recharge a lithium ion battery.

Nuclear Power

Viking 1 and 2 had radio-isotope thermal generator units containing plutonium 238. Each generator had a mass of 13.6 kg and provided continuous power at 30 W. Such power-to-weight ratios are unsuitable for MARV.

Fuel Cells

Fuel cells are electrochemical devices that convert chemical energy of a reaction directly into electrical energy. A fuel cell can produce electricity, water, and heat from a fuel and an oxidant. According to AeroEnvironment, Inc., fuel cell systems would readily store 400 W·h/kg, and they are targeting a value of 600 W·h/kg for powering the long endurance aircraft Helios.[16] With these values only 5–10 kg of fuel cell system is required. Fuel cells may be classified by the type of electrolyte they use. Polymer electrolyte fuel cells or proton exchange membrane fuel cells (PEM) use a proton conducting hydrated ion exchange membrane. Operating temperatures are low and around 80°C (Ref. 17).

Alkaline fuel cells use concentrated (85% by weight) potassium hydroxide (KOH) or less concentrated KOH (35–50%) (Ref. 17). Operating temperatures are around 250°C. The Martian atmosphere is rich in CO_2, and a small leak in the cells will quickly form potassium carbonate K_2CO_3, bringing the entire system to a halt. Phosphoric acid fuel cells use concentrated to 100%, phosphoric acid as electrolyte. This kind of cell operates at temperatures of 150–220°C (Ref. 17) Molten carbonate fuel cells use a combination of alkali carbonates or of sodium and potassium and are retained in a ceramic matrix of lithium aluminum oxide. This is a very high-temperature cell operating at 600–700°C (Ref. 17) and is unsuitable for use on Mars. The electrolyte in solid oxide fuel cells (SOFC) is a solid, non porous metal oxide. SOFC is also a high-temperature cell operating at 650–1000°C (Ref. 17).

MARV Power Plant

Based on this study, fuel cells are selected for MARV power plant. Fuel cells provide minimum system weight with currently proven technology on Earth. They are reliable, environmentally clean, and have good growth potential. They can provide means of conducting multiple missions in future by using regenerative techniques.[16] Batteries and solar cells used together are the second option.

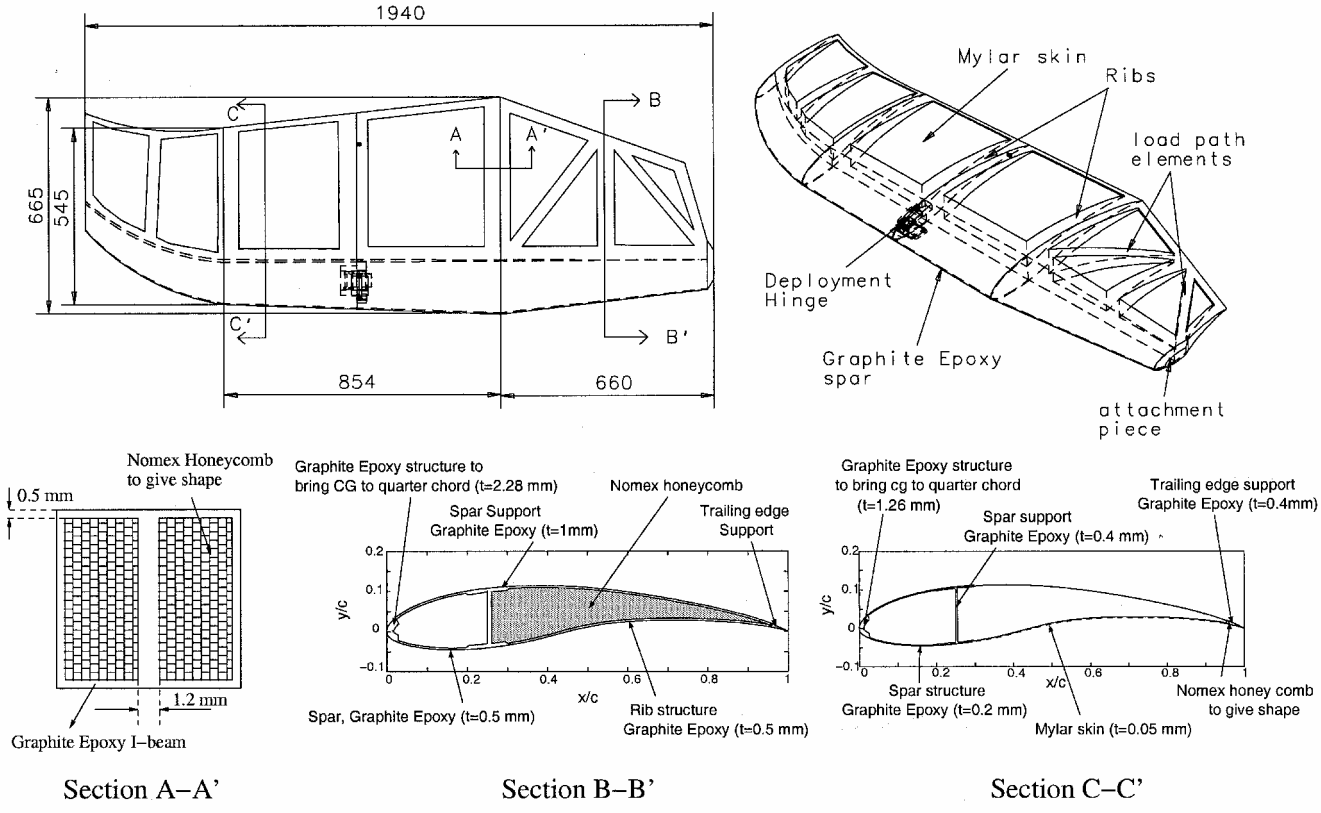

Fig. 12 Structural design of MARV blade.

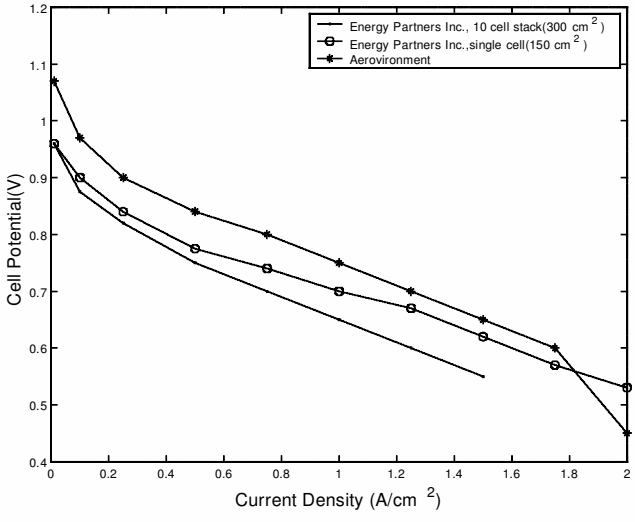

Fig. 13 Performance of PEM fuel cells.

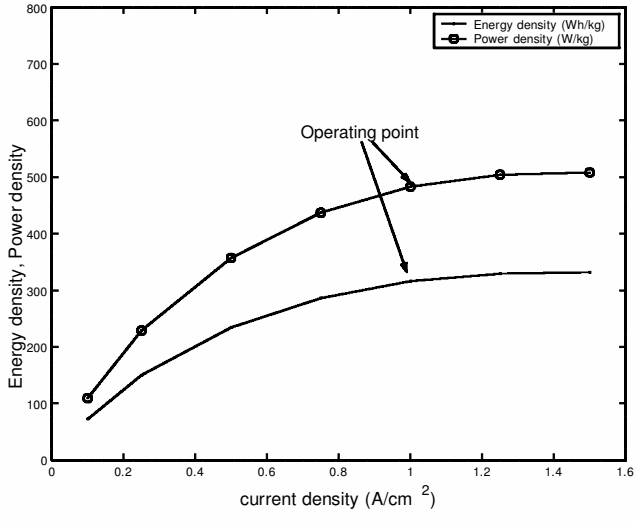

Fig. 14 Energy density and power density of PEM fuel cell system as a function of operating condition.

Although they reduce the payload capability by 10 kg, they offer multiple-mission capability.

PEM fuel cells are chosen for MARV with pure oxygen and pure hydrogen as fuel. Their low-temperature operation, faster start ups, and quick response to changes in power demand are best suited for use in low-temperature Martian environment. With pure reactant, higher power densities can be achieved. The fuel cell system designed for MARV consists of the fuel cell stack, fuel tanks, thermal and water management units, and ancillary control equipment. Polarization curves of PEM fuel cells are shown in Fig. 13. Current density, which is current flowing through each cell divided by the active area of the cell, increases with decrease in cell potential. The curves from Energy Partners, Inc., are obtained with a hydrogen–air single cell and a 10 cell stack at 60°C. The AeroVironment curve is for a pure hydrogen, pure oxygen fuel cell.[16] Multicell performance results of Energy Partners, Inc., is used in the present design to allow a comfortable technology margin.

The fuel cell stack is designed for an average power output of 4.63 kW. The voltage output from the stack is 188 V sufficient for the electric motors, avionics, controls, and payload. The thickness of each cell is taken as 4400 μm. Each cell has a density of 2500 kg/m^3 with porosity of 60%. Hydrogen and oxygen utilization are assumed 100%. For pure fuels, this is a realistic assumption. Masses of fuel required, fuel stack, and tanks have been estimated for different combinations of cell voltages and current densities. Efficiency of electric motor is 90%. System mass is calculated for different combinations of cell voltages and current densities.

Corresponding to each system mass, the energy densities and the power densities of the fuel cell system, for the basic mission, are plotted in Fig. 14. From this curve, the operating point of a cell is

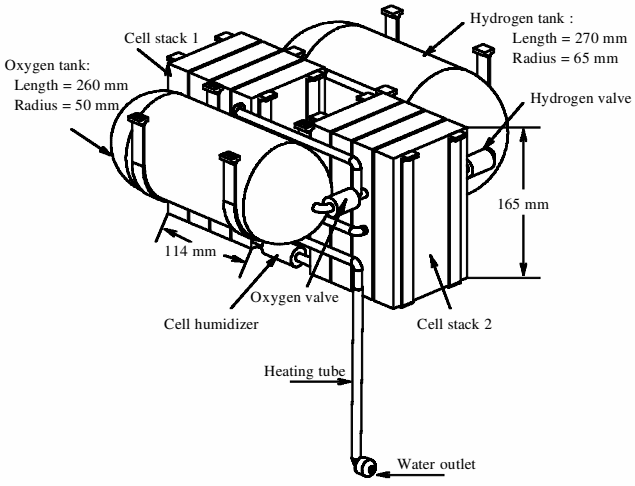

Fig. 15 MARV power plant: PEM fuel cell system.

chosen to be 0.65 V and 1 A/cm^2. This combination provides energy density and power density values close to the maximum without pushing the cells to their limit. As a result, it provides adequate margin for current density during higher power consumption at hover. The energy density and power density of the system in case of the extended mission becomes 350 W·h/kg and 452 W/kg. The maximum power output capacity is 6.43 kW. The fuel cell uses pure hydrogen and pure oxygen as reactants. The required masses of hydrogen and oxygen for the entire mission are 0.23 and 1.83 kg, respectively. Hydrogen and oxygen are stored in tanks at cryogenic temperatures and supercritical pressures. They flow into the stacks through relief valves. A fuel oxidant method of cooling is used. Byproduct water produced is collected in an intermediate water chamber from where the excess is thrown out. If water is needed for humidization, it is taken from the water chamber. The layout of the fuel cell system is shown in Fig. 15.

Electric Motor and Transmission

The output of the power plant is used to run a brushless dc electric motor. The motor chosen in the present design is built by the Aveox Company. It produces the required torque at 11,500 rpm with a 160-V dc, 34.2-A input. The angular velocity of the motor can be controlled by the average voltage applied to the winding. The motor speed can be measured by an ac tachometer generator whose induced voltage magnitude and frequency is a measure of the speed.

The transmission provides a 18:1 reduction ratio from the electric motor to the rotor. The transmission system configuration is based on four critical considerations: weight, compactness, ease of gears and bearing installation, and implementation of yaw control. Figure 16 shows the transmission design. It uses two-stage planetary gears for speed reduction and internal gears to achieve dual rotation of the coaxial shafts.

Control System Design

Four control concepts are examined for MARV. These are 1) plain/servo flaps, 2) moving tip, 3) shaft tilt control, and 4) swashplate control. At low Reynolds number, a flap remains completely submerged in the thick boundary layer and has limited effectiveness. Additionally, there is a possibility of completely destroying the flow because at low Reynolds numbers the flow is extremely sensitive to disturbances. Also, a moving tip presents problems during folding, due to the bending–torsion coupled beam that runs along the span. Neither shaft tilt nor c.g. shift provides sufficient collective or yaw control authority. Hence, swashplate control is the most reliable option on Mars.

MARV Control System

A coupled collective-yaw control mechanism is designed for MARV. When the collective is applied, both the rotors have the same pitch input. When the yaw control is applied, the top rotor has the same pitch input as the bottom rotor, but in the opposite direction. Figure 17 shows the detailed mechanism.

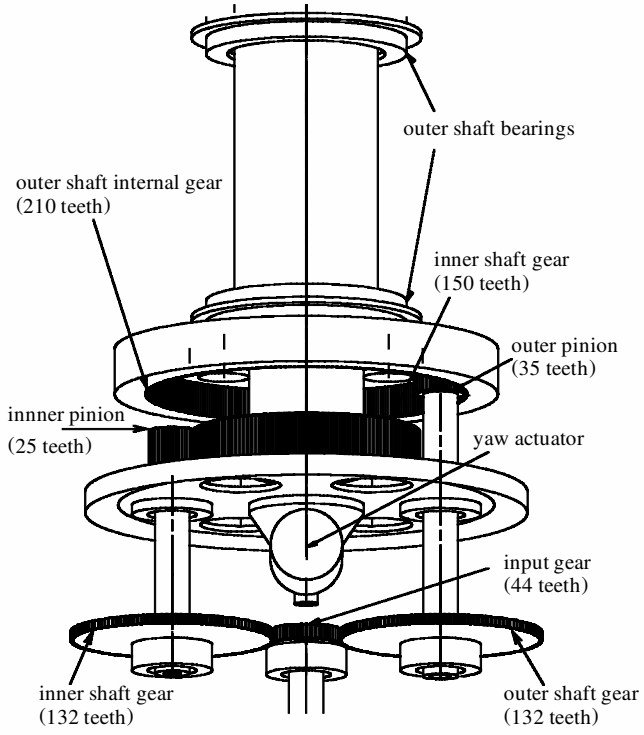

Fig. 16 MARV transmission.

The collective-yaw control is implemented using two motions: 1) vertical motion of the swashplates and 2) vertical motion of the yaw control linkage. The two swashplates are connected and have identical vertical motions. The yaw control linkage is a rod that can slide up and down through the inner shaft. It is fixed to the rigid frame ABA′C′C at point B (Fig. 17). The frame is connected to two forks, EFGG′ and E′F′GG′. Note that G′ and F′ are hidden in Fig. 17. The motion of the yaw control linkage is directly transmitted to point G (and G′) via the rigid frame. The motion of the swashplates is directly transmitted to F via the linkage FH (and F′H′).

When the collective control is applied, the yaw linkage is given the same vertical displacement as the swashplates. As a result, both G and F (also G′ and F′) have the same vertical displacement (Fig. 17). This is transmitted to the pitch link DE (and D′E′) at point E (and E′). Thus, the pitch angle of the top and bottom rotors change by the same amount.

When the yaw control is applied, the yaw linkage is given three times the vertical displacement of the swashplates. As a result, while G (and G′) moves vertically by three units, F (and F′) moves vertically by one unit (Fig. 17). The length EF (and E′F′) is designed to be the same as length GF (and G′F′) so that the pitch link DE (and D′E′) move by one unit in the opposite direction to the swashplate input. Thus, the pitch angle of the top and bottom rotors change by the same amount, but in opposite directions. When the total thrust is kept constant, a differential torque is generated for yaw control.

Fuselage and Landing Gear Design

Fuselage

The fuselage structure is a rigid hexahedral. It consists of two rectangular horizontal frames connected by four vertical struts and supported on each side by two cross struts for torsional stiffness. A thin skin of Mylar is used to cover the fuselage. The fuselage design is shown in Fig. 18. Inside the fuselage, the equipment is arranged in two stages: one upper stage for the power system and one lower stage for the avionics and payload. The fuel, oxidizer, and water circuits are so arranged that the c.g. is exactly placed on

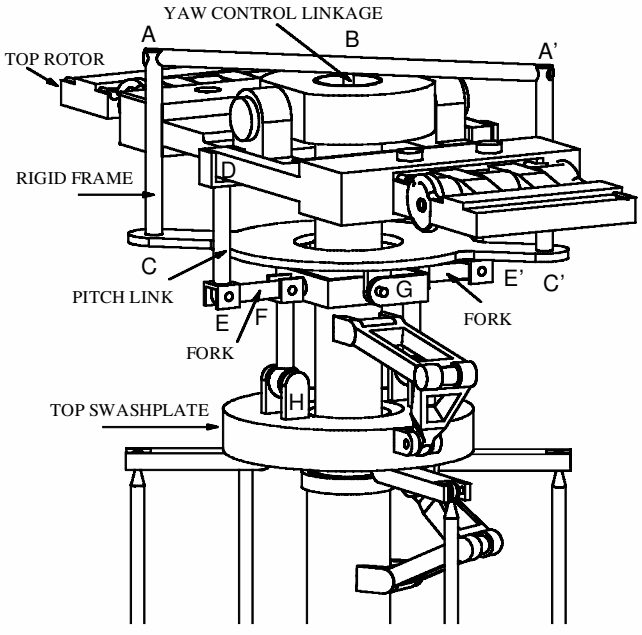

Fig. 17 MARV control system: coupled collective-yaw swashplate control note that points F′, G′, and H′ are hidden.

the shaft axis. Because the payload can be of many types, no fixed payload bay is designed, but a space is kept under the avionic box ($150 \times 350 \times 360$ mm^3), and four attachment points are provided on the lower frame.

Gear-Box Suspension

The gear box is attached to the structure at two levels (Fig. 19): at the rotor mast level by four V-shaped struts, transmitting the rotor lift to the structure (each strut is V-shaped to ensure torsional strength), and at the gear-box level by a flexible suspension, placed between the bottom of the gear-box-motor assembly.

The four rigid struts are attached to the rotor mast and the fuselage using ball bearings. Suspended like a pendulum, the gearbox oscillates around the meeting point of the four suspension bars. The principal part of the flexible suspension is a cylindrical element formed by a succession of thin disks of rubber and duralumin, as shown in Fig. 19. One face of each element (four elements in total) is bonded to the gear box, whereas the other is bonded to the structure. The vibration absorption occurs in the radial direction of the element, deformed in shear. The reaction couple from the motor is taken in compression by all four elements. This vibration absorption device is designed to cancel the in-plane vibrations induced by the high lag frequency.

Landing Gear

A deployable, four-legged landing gear is designed. Each leg has an articulated foot pad containing crushable aluminum honeycomb. The foot pads (110 mm diam) are articulated to allow the vehicle to adapt to slopes and rocks. The folding linkage design achieves a retraction ratio of almost 80%. MARV rotors are stiff in-plane, with a lag frequency of 3.7 per revolution. Hence, ground resonance is not encountered.

The folding linkages consist of three articulated leg sections retracting along the fuselage, as shown in Fig. 18. Each leg consists of three parts: one primary strut, articulated around a hinge for retraction, and two secondary struts attached to two contiguous sides of the fuselage. The folding hinge on the primary strut is equipped with a torsion spring. In the retracted position, the spring is compressed. When the link is released, the spring extends the two parts of the primary strut in a colinear position. The size of the landing legs is determined by the Federal Aviation Regulations 29.725 requirement stating that the vehicle should withstand a drop test of 8 in., with a 1.5 safety factor. This corresponds to a drop velocity on

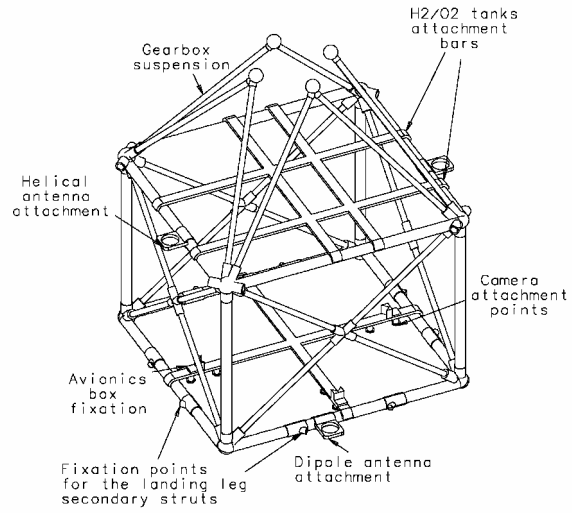

a) Fuselage structure

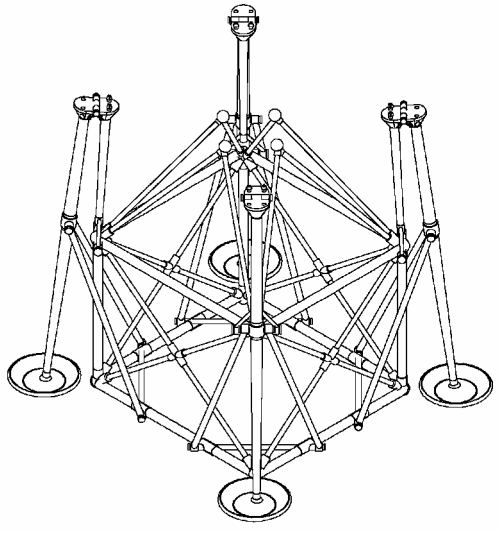

b) Retracted landing gear

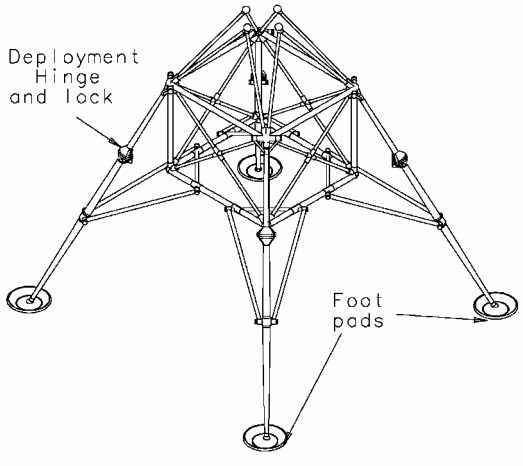

c) Deployed landing gear

Fig. 18 Fuselage and landing gear design.

Mars of 1.5 m/s (4.9 ft/s). Each leg is designed to sustain this drop test without permanent deformation.

The c.g. of MARV has 0.06% rotor radius longitudinal offset and 0.3% lateral offset. Table 4 shows the final weights of the major components of MARV. Payload occupies the highest weight fraction (21.6%), followed by power plant (30%, including electric motor, fuel and drive system). In comparison, a helicopter on Earth has a payload fraction of 35–40% and power plant fraction of 20% (including fuel, engine, and drive system). MARV fuselage is lighter

(6.8% compared to 15% on Earth) but the rotor system (blades, hub, and control system) is heavier (27% compared to 10% on Earth).

MARV Deployment

Each rotor blade is folded twice to make the vehicle as compact as possible. The entire deployment scheme is shown in Fig. 20.

Step 1 shows the lander after touchdown on Mars. In step 2, the four lander petals open. The cords attached to the wider petals unspool freely. In step 3, the cords are pulled in by winches drawing out the outboard sections of the blades to prevent interference in the following step. In step 4, the inboard sections of the blades are deployed. Attachments to the lander base are released, and torsion springs located at the root of each blade deploy and lock the blade in place. Next, the wider petals open out farther. The winches unwind, and the cords unspool freely. This is shown in step 5. In step 6, the cords are pulled in. The outboard sections of the blade unfold, and when they become colinear, a pawl latch mechanism locks them into position. Finally in step 7, the attachment clips of the cords to the tip of each blade are released. The helical antennas are deployed. MARV is ready to start. Step 8 starts the rotors and detaches the structural attachments of MARV to the lander. When MARV takes off, the power system is switched to the fuel cells, and electrical connections to the lander are detached. After takeoff, the landing gears are extended by torsion springs and locked into place by pawl latches. This is shown as the last step 9. Finally, the helicopter transitions into forward flight.

Table 4 Weight break up of MARV components

Parameter	Mass, kg	% Gross takeoff weight
Fuselage	3.4	6.8
Motor	2.0	4.0
Power supply	10.6	21.1
Blades	6.0	12.0
Hub	3.3	6.5
Control group	4.1	8.1
Drive system	2.2	4.4
Landing gear	3.6	7.2
Avionics	4.1	8.2
Payload	10.8	21.6
Gross weight	50	100

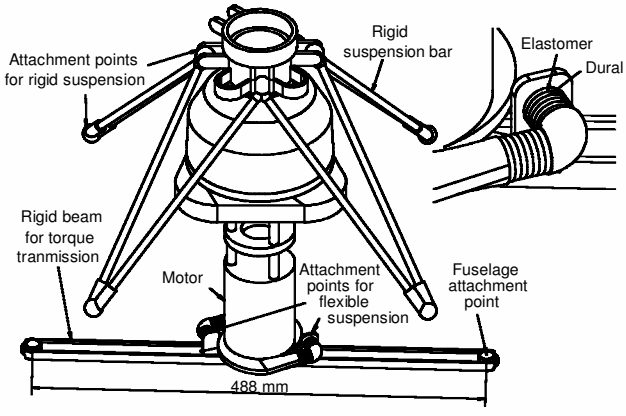

Fig. 19 Gear-box suspension.

Vehicle Lander Communications

Mars is an isolated environment with no satellites in orbit, no repeater stations on ground, and no significant ionosphere to bounce off signals. MARV uses one omnidirectional vertical dipole antenna to receive signals and two helical directional antennas to transmit signals. line-of-sight (LOS) contact is maintained with the lander. The horizon falls off at an increased rate of 7 in./mile on Mars (4 in./mile on Earth). A 2.76-m-high lander antenna is needed to keep LOS contact.

The transmission frequency is chosen at 2.4 GHz. A low transmission frequency is chosen to minimize path losses in signal power. With a frequency of 2.4 GHz and a transmission distance of 25 km, path loss is 128 dB. Omnidirectional antennas are simple (approximately 0.002 kg each) but have low gains (0–5 dB). When a gain of 5 dB is assumed, the signal strength at the receiver would be −113.5 dB, which is an unacceptable bit error rate (BER). An acceptable BER is around −80 dB. Helical directional antennas require actuators and tracking systems to maintain LOS contact (approximately 0.3 kg per system) but they have high gains (6–30 dB) and low path losses. MARV uses helical directional antennas for the primary means of transmission. In case of failure, the omnidirectional antenna can still be used. Thus, a failure of the directional antenna will not result in a total mission failure.

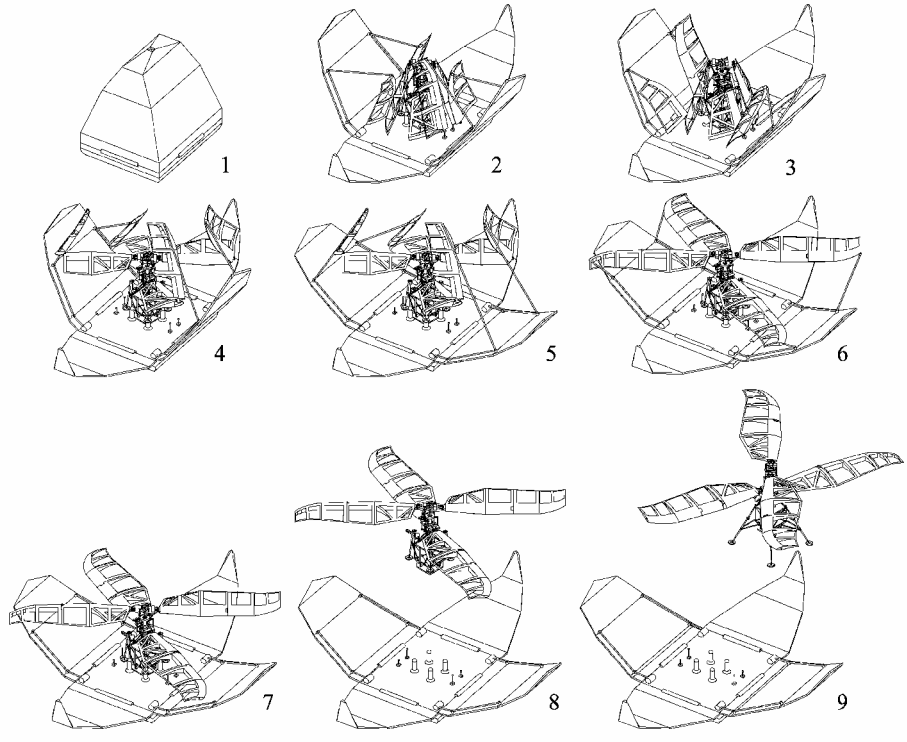

Fig. 20 MARV deployment from lander on Mars.

Avionics components are packaged inside thermally insulated boxes using solid-silica insulator aerogel, similar to Sojourner.[18] Three outboard avionics boxes each contain a pressure transducer, a temperature probe, and a camera. The inboard avionics box contains the flight and data computer, data multiplexer, radio transceiver, temperature sensor, three gyros, and a compass. The outboard avionics measure flight conditions such as altitude, rate of climb and flight speed, and inputs to the flight computer. The inboard avionics maintain trim and course, store and transmit data, and maintain proper internal environment. The mission profile and point-specific commands are preset into the flight computer. Based on in-flight measurements, it adjusts course and trim autonomously. The complete avionics and communication system has a mass of 4.07 kg and operates at an average power of 62 W.

Summary

The preliminary design of MARV has been presented. MARV has an unconventional rotor planform, which resembles a propeller blade more than a rotor blade on Earth. Airfoil AGRC 1506 has been specially designed to provide adequate flying capabilities. MARV has a coaxial rotor system with teetering hub and a swashplate-based coupled collective-yaw control system. Fuselage design includes optimal placement of subsystems and a scientific payload bay. MARV has retractable landing gears. Helical directional communicatian antennas maintain LOS communication between MARV and the lander. Special care is taken to design a folding mechanism that fits MARV inside the dimensions of the Mars polar lander (1998). A detailed deployment mechanism is developed to deploy MARV on Mars. Based on the design exercise, the following conclusions have been made.

1) Controlled vertical takeoff landing flight on Mars is feasible with existing technologies.

2) It is necessary to maintain blade chord Reynolds numbers above 5×10^4 to fly a helicopter on Mars. Below 5×10^4 high adverse pressure gradients resulting from high blade loading separates the turbulent boundary layer easily. MARV blades maintain blade chord Reynolds numbers above 5×10^4 over 60% of the span.

3) Forward flight speed on Mars is limited by airfoil critical Mach numbers that take place at the retreating blades due to high lift (not at advancing blades). Because of low Reynolds numbers, there exists no margin between critical Mach number and drag divergence Mach number. Even a weak shock completely separates the flowfield. Together with a low speed of sound, steep pressure peaks due to high blade loading bring about critical conditions at low speeds (20 kn).

4) Currently used airfoils are not suited for a Martian helicopter. Existing low Reynolds number airfoils are point designs and suited for low Mach number operations. Therefore, AGRC 1506 has been designed for MARV to provide efficient performance over a range of low Reynolds numbers (5×10^4–1×10^5) and moderate Mach numbers (subsonic–0.5).

5) Airfoils with high camber appear necessary for Martian flight. Because of low values of dimensional pitching moments, control loads encountered are not high.

6) A coaxial helicopter configuration is more suited for a Martian mission. It can be tailored to produce chord Reynolds numbers and Mach numbers necessary for efficient airfoil operation in restrictive Martian conditions. It is suited for compact stowage.

7) Reynolds number and Mach number requirements lead to high aspect ratio blades (around 4), which resemble propeller blades on Earth. Low aspect ratio blades lead to rotors that are comparatively stiff. A teetering hub is simple and free from instabilities. It transfers no vibratory moments to the fuselage. In-plane vibration is effectively isolated from sensitive instruments through vibration absorbers in the gear-box suspension.

8) There exists no feasible technology for in situ propellant production on Mars, which might reduce takeoff weight. Multiple missions are possible only by replenishing an onboard rechargeable battery, using solar cells on the lander. With absorption rates noted during the Pathfinder/Sojourner mission, mission energy can be replenished in a little over three days. However, payload capability is only 0.8 kg.

9) For high payload, sample-return-type missions achieved in MARV, a PEM-type power plant is most suitable. However, cryogenic storage over a long period of time (two years to reach Mars) requires further investigation. Regenerative techniques for fuel cell recharge are attractive for multiple mission capability. Although such techniques exist for hydrogen–oxygen fuel cells,[18] the process of pressurizing the gases back into the storage tanks under cryogenic conditions has severe weight penalty.

10) At low Reynolds numbers, a conventional swashplate provides the best means of primary rotor control as opposed to low weight flaps or moving tips.

11) Most stringent loads for vehicle structural design come from atmospheric deceleration.

12) Large variations in temperature (year round variation from -132.6 to 17.4°C, diurnal variation from 0 to -100°C) are found on Mars. However, most composites, aluminum, and titanium alloys can be readily used for structural design. Low-temperature lubricants such as Bray grease 604 (used in Sojourner) can be used for transmission.

MARV incorporates an innovative utilization of currently proven technology on Earth, with minimal reliance on future extrapolation. MARV is a feasible design. It is a safe, reliable and ideal candidate for being a natural extension of a ground-based robotic vehicle on Mars.

Acknowledgments

The authors thank NASA Ames Research Center (Larry Young) and Sikorsky Aircraft Corporation for organizing this challenging and unique design competition. The authors are grateful to the following people for their active support, collaboration, and consultancy during the design project: Marat Tishchenko (Academician of the Russian Academy of Science), Inderjit Chopra, Alfred Gessow, and V. T. Nagaraj. In addition, the authors would like to thank Greg Jackson, Gordon Leishman, Mark Lewis, Preston Martin (University of Maryland) and Mark Drela (Massachusetts Institute of Technology) for useful discussions.

References

[1]Young, L., Chen, R., Aiken, E., and Briggs, G., "Design Opportunities and Challenges in the Development of Vertical Lift Planetary Aerial Vehicles," *Proceedings of the American Helicopter Society Vertical Lift Aircraft Design Specialist's Meeting*, San Francisco, CA, Jan. 2000, pp. 1–23.

[2]Young, L., "Vertical Lift—Not Just for Terrestrial Flight," American Helicopter Society/AIAA/Royal Aeronautical Society/Society of Automotive Engineers, International Powered Lift Conf., Arlington, VA, Oct.–Nov. 2000, pp. 1–25.

[3]Savu, G., Oprisiu, C., and Trifu, O., "An Autonomous Flying Robot for Mars Exploration," 44th Congress of the International Astronautical Federation, Oct. 1993, Austria.

[4]Datta, A., Roget, B., Griffiths, D., Pugliese, G., Sitaraman, J., Bao, J., Liu, L., Gamard, O., and Chopra, I., "Design of a Martian Autonomous Rotary-Wing Vehicle," *Design Report*, submitted to the American Helicopter Society, Winner of 17th AHS Student Design Competition, June 2000, pp. 1–97.

[5]Stepniewski, W. Z., and Shinn, R. A., "A Comparative Study of Soviet vs. Western Helicopters: Part II, Evaluation of Weight, Maintainability, and Design Aspects of Major Components," NASA CR 3580, March 1983.

[6]Giguere, P., and Selig, M. S., "Low Reynolds Number Airfoils for Small Horizontal Axis Wind Turbines," *Wind Engineering*, Vol. 21, No. 6, 1997, pp. 367–380.

[7]Greer, D., Hamory, P., Krake, K., and Drela, M., "Design and Predictions for a High-Altitude (Low-Reynolds-Number) Aerodynamic Flight Experiment," NASA TM-1999-206579, July 1999.

[8]Evangelista, R., McGhee, R., and Walker, B., "Correlation of Theory to Wind-Tunnel Data at Low Reynolds Numbers Below 500,000," *Low Reynolds Number Aerodynamics, Lecture Notes in Engineering*, Springer-Verlag, New York, 1989, No. 54, p. 146.

[9]Drela, M., "Low Reynolds Number Airfoil Design for the Massachusetts Inst. of Technology Daedalus Prototype: A Case Study," *Journal of Aircraft*, Vol. 25, No. 8, Aug. 1988, pp. 724–732.

[10]Akkerman, J. W., "Hydrazine Monopropellant Reciprocating Engine Development," NASA CP 2081, 13th Aerospace Mechanisms Symposium, Houston, TX, April 1979, pp. 1–14.

[11] Hill, P., and Peterson, C., *Mechanics and Thermodynamics of Propulsion*, 2nd ed., Addison–Wesley, Reading, MA, 1992, pp. 571–575.

[12] Yuasa, S., Sogo, S., and Isoda, H., "Ignition and Combustion of Aluminium in Carbon Dioxide Streams," *Proceedings of the 24h International Symposium on Combustion*, Pittsburgh, PA, July 1992, pp. 1817–1825.

[13] Vincent, C., and Scrosati, B., "Modern Batteries: An Introduction to Electrochemical Power Sources," 2nd ed., Wiley, New York, 1997, pp. 141, 199.

[14] Partain, L., "Solar Cells and Their Applications," Wiley, New York, 1995, pp. 361–388.

[15] Stevenson, S., "Mars Pathfinder Rover-Lewis Research Center Technology Experiments Program," NASA TM-107449, July–Aug. 1997.

[16] Dornheim, M., "Special Fuel Cells Key to Month-Long Flight," *Aviation Week and Space Technology*, Feb. 2000.

[17] Hirschenhofer, J. H., Stauffer, D. B., Engleman, R. R., and Klett, M. G., *Fuel Cell Handbook*, 2nd ed., Rept. DOE/FETC-99/1076, Dept. of Energy, 1998.

[18] Matijevic, J., "Sojourner: The Mars Pathfinder Microrover Flight Experiment," *Space Technology*, Vol. 17, No. 3–4, May–July 1997, pp. 143–149.